Neural Networks 23 (2010) 752–763

Contents lists available at ScienceDirect

Neural Networks

journal homepage: www.elsevier.com/locate/neunet

2010 Special Issue

Bayesian estimation of phase response curves

Ken Nakae [a,*], Yukito Iba [b], Yasuhiro Tsubo [c], Tomoki Fukai [c], Toshio Aoyagi [d]

[a] Department of Statistical Science, School of Multidisciplinary Sciences, The Graduate University for Advanced Studies, 10-3, Midori-Machi, Tachikawa, Tokyo, 1068569, Japan
[b] Department of Statistical Modeling, The Institute of Statistical Mathematics, 10-3, Midori-Machi, Tachikawa, Tokyo, 1068569, Japan
[c] Laboratory for Neural Circuit Theory, Brain Science Institute, RIKEN, 2-1, Hirosawa, Wako, Saitama 3510198, Japan
[d] Department of Applied Analysis and Complex Dynamical Systems, Graduate School of Informatics, Kyoto University, Yoshida-Honmachi, Sakyo-ku, Kyoto, 6068501, Japan

ARTICLE INFO

Article history:
Received 20 October 2009
Revised and accepted 10 April 2010

Keywords:
Synchronization
Phase response curve
Bayesian framework
Markov chain Monte Carlo
Replica exchange Monte Carlo

ABSTRACT

Phase response curve (PRC) of an oscillatory neuron describes the response of the neuron to external perturbation. The PRC is useful to predict synchronized dynamics of neurons; hence, its measurement from experimental data attracts increasing interest in neural science. This paper introduces a Bayesian method for estimating PRCs from data, which allows for the correlation of errors in explanatory and response variables of the PRC. The method is implemented with a replica exchange Monte Carlo technique; this avoids local minima and enables efficient calculation of posterior averages. A test with artificial data generated by the noisy Morris–Lecar equation shows that the proposed method outperforms conventional regression that ignores errors in the explanatory variable. Experimental data from the pyramidal cells in the rat motor cortex is also analyzed with the method; a case is found where the result with the proposed method is considerably different from that obtained by conventional regression.

1. Introduction

Synchronization between neurons is observed everywhere in neural systems (Salinas & Sejnowski, 2001; Varela, Lachaux, Rodriguez, & Martinerie, 2001). For example, the periodic activities seen in EEG are regarded as evidence of synchronicity in the brain. Gray and Singer (1989) proposed a hypothesis that synchronization is essential for understanding the "binding problem" in cognitive neuroscience. Fries (2005) introduced the "communication through coherence" hypothesis, which suggests that coherent oscillations of neurons are important for information transmission in the brain. These hypotheses argue that coherence in neural activities induced by synchronization is not a side effect but essential for understanding brain functions.

To deal with synchronization from the theoretical viewpoint, Kuramoto (1984) developed a theory based on the phase description of an oscillator; see also Ermentrout (1996), Hansel, Mato, and Meunier (1995), Izhikevich (2007), Kopell and Ermentrout (1990), Winfree (2001), and recent surveys (Acebrón, Bonilla, Pérez Vicente, Ritort, & Spigler, 2005; Strogatz, 2000). A key concept of this theory is the phase response curve (PRC), which describes the response of an oscillator to external perturbations. According to the studies by Kuramoto and his successors, the PRC and the network topology are two essential features that determine the synchronicity of an oscillator network. In terms of neural science, neuron's PRCs can be useful for reconstructing the properties of a network consisting of neurons.

Many researchers have recently tried to estimate neuron's PRCs from experimental data (Ermentrout, Galán, & Urban, 2007; Ermentrout & Saunders, 2006; Galán, Ermentrout, & Urban, 2005; Goldberg, Deister, & Wilson, 2007; Gutkin, Ermentrout, & Reyes, 2005; Netoff et al., 2005; Ota, Nomura, & Aoyagi, 2009; Preyer & Butera, 2005; Tsubo, Takada, Reyes, & Fukai, 2007). Noise in the PRC measurements is often very large, and sophisticated statistical techniques are necessary for efficient estimation. A typical method used in these studies is fitting the data with a linear combination of trigonometric functions. Ota and co-workers (Aonishi & Ota, 2006; Ota, Omori, & Aonishi, 2009) introduced a Bayesian procedure wherein PRCs are assumed to be smooth functions. The Bayesian approach has the advantage of easily introducing prior information on PRCs as well as on the measurement process.

A common weakness of the previous studies is that they neglect the errors in the PRC explanatory variables. They also neglect the correlation between errors in the explanatory and response variables; the significance of this correlation is discussed in Section 2.2. This study is devoted to developing a new method that can deal with these errors and the correlation through a systematic use of Bayesian methods. Unlike previous Bayesian methods (Aonishi & Ota, 2006; Ota et al., 2009), our method does not require an assumption that the timing of a perturbation represented as a phase,

* Corresponding author. Tel.: +81 05055338524; fax: +81 0425264335.
E-mail addresses: nakae@ism.ac.jp (K. Nakae), iba@ism.ac.jp (Y. Iba), yasuhirotsubo@riken.jp (Y. Tsubo), tfukai@riken.jp (T. Fukai), aoyagi@acs.i.kyoto-u.ac.jp (T. Aoyagi).

0893-6080/$ – see front matter © 2010 Elsevier Ltd. All rights reserved.
doi:10.1016/j.neunet.2010.04.002

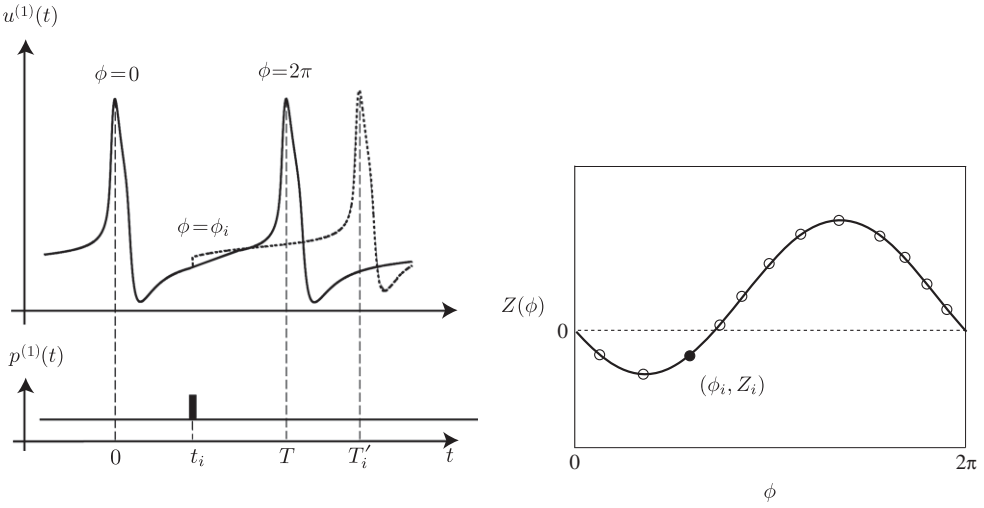

Fig. 1. Measurement of a phase response curve. A trial with a perturbation at $t = t_i$ is illustrated in the left panel. The solid curve indicates the voltage for the neuron without perturbation, while the dotted curve indicates the voltage with perturbation. Each point (ϕ_i, Z_i) in the right panel corresponds to a trial with timing t_i. The PRC is defined by interpolating these points.

later defined as ϕ_i in (1), is known exactly. Using the proposed procedure, we successfully improved the estimation precision for PRCs in examples of simulated data. The proposed method is also applied to experimental data from the pyramidal cells in the rat motor cortex.

The role of errors in explanatory variables for regression has been considered in the literature on statistics (Amari & Kawanabe, 1997; Berry, Carroll, & Ruppert, 2002; Caroll, Ruppert, Stefanski, & Crainiceanu, 2006; Cheng & Ness, 1999; Fuller, 1987). The correlation between errors in the explanatory and response variables is also treated in some textbooks, for example, Cheng and Ness (1999), but it seems a less known subject; its appearance in the present problem of estimating PRCs will be interesting in terms of statistical science.

The Bayesian model proposed in this paper is nonlinear and non-Gaussian; a standard way to treat such a model is with Markov chain Monte Carlo (MCMC) methods (Gelman, Carlin, Stern, & Rubin, 2003; Gilks, Richardson, & Spiegelhalter, 1995; MacKay, 2003; Robert & Casella, 2004). For the current problem, however, a direct application of standard MCMC methods is difficult due to the slow convergence of MCMC. To deal with this difficulty, we introduce the replica exchange Monte Carlo (REM) method (Geyer, 1991; Hukushima & Nemoto, 1996; Iba, 2001). The REM is widely used in statistical physics and biomolecular simulations, and also applied to statistical inference (Geyer & Thompson, 1995; Huelsenbeck & Ronquist, 2001; Jasra, Stephens, & Holmes, 2007). Using the REM, the difficulty is reduced, and we can get results within a reasonable amount of time.

The proposed method for PRC estimation is useful for any kind of nonlinear oscillator that permits the phase description. Although our current interest is in applications for brain science, this method can also be used in other fields of biology, chemistry, and physics.

The organization of this paper is as follows: in the next section, we define the PRC and discuss the properties of the correlation between errors in the explanatory and response variables. In Section 3, we propose a Bayesian model where we consider both the correlation of errors and smoothness of PRCs. In Section 4, we discuss how to estimate the PRC from data using the REM. In Sections 5 and 6, we test the proposed procedure with artificial data generated using the Morris–Lecar equation (Morris & Lecar, 1981) and data from a real experiment.

2. Phase response curve

2.1. Definition of the phase response curve

First, we define the PRC of a neuron from an operational viewpoint. We assume that the activity of a neuron is periodic and that the period is T. The solid curve in the left panel of Fig. 1 represents the voltage time-series for the neuron. We consider a set of trials indexed by i. The neuron is assumed to fire at the origin $t = 0$. For the ith trial, a perturbation is added at time $t = t_i$. The neuron then fires again at time $t = T_i'$ as shown by the dotted curve in Fig. 1. We repeat this procedure a number of times and plot the points $(\phi_i, Z_i),\ i = 1, \ldots, n$, defined by

$$\phi_i = 2\pi \frac{t_i}{T}, \qquad Z_i = 2\pi \frac{T - T_i'}{T}. \tag{1}$$

The curve $Z(\phi)$ interpolating these points is the phase response curve (PRC) of the neuron and is shown by the solid curve in the right panel of Fig. 1.

Next, we discuss a connection to the theory of dynamical systems. Let us represent the state of a neuron by the vector $\mathbf{u} = (u^{(1)}, \ldots, u^{(m)})$, whose first component $u^{(1)}$ corresponds to the voltage of the neuron. An equation that describes dynamics of the neuron is assumed as

$$\frac{\mathrm{d}\mathbf{u}}{\mathrm{d}t} = \mathbf{F}(\mathbf{u}) + \mathbf{p}(t), \tag{2}$$

where the vector $\mathbf{p}(t) = (p^{(1)}(t), \ldots, p^{(m)}(t))$ represents external perturbation. Hereafter, the vector field $\mathbf{F}(\mathbf{u})$ is assumed to have a stable limit cycle. If the perturbation $\mathbf{p}(t)$ is sufficiently small, Eq. (2) is reduced to

$$\frac{\mathrm{d}\phi}{\mathrm{d}t} = \frac{2\pi}{T} + \mathbf{Z}(\phi) \cdot \mathbf{p}(t), \tag{3}$$

where a point on the limit cycle is indicated by the phase variable $\phi \in [0, 2\pi)$ (Kuramoto, 1984). Eq. (3) suggests that a neuron is characterized by the function $\mathbf{Z}(\phi) = (Z^{(1)}(\phi), \ldots, Z^{(m)}(\phi))$.

When the perturbation $\mathbf{p}(t)$ is added to the first component $u^{(1)}$ only and the functional form of $p^{(1)}(t)$ is Dirac's delta function $\delta(t - t_i)$, Eqs. (2) and (3) correspond to the experiment defining PRCs from the operational viewpoint. Thus, we can identify the function in Eq. (3) with a PRC $Z(\phi)$ defined from the operational viewpoint. The vector function $\mathbf{Z}(\phi)$ in Eq. (3) can be regarded as a

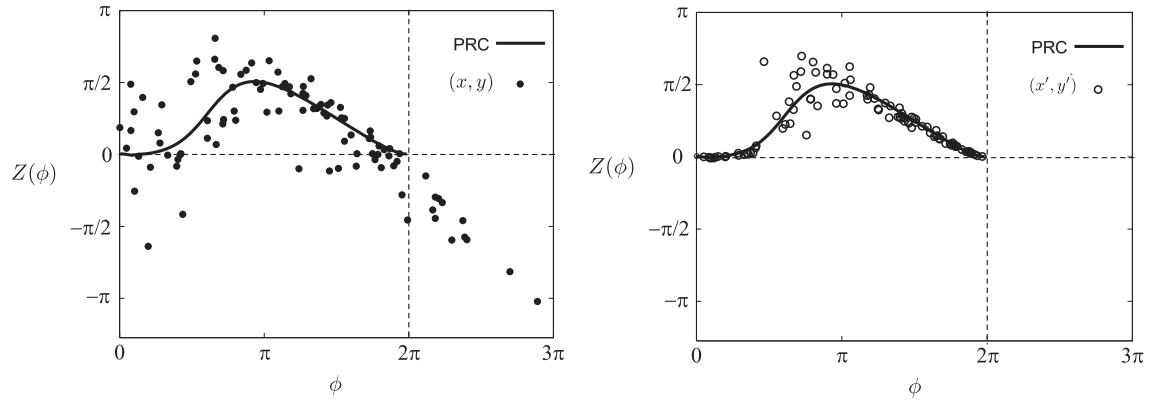

Fig. 2. Comparison of the different normalization schemes. The left and right panels correspond to Eqs. (4) and (5), respectively.

generic definition of the PRC. Hereafter, we deal with $Z^{(1)}(\phi)$, the PRC of membrane potential, and denote it by $Z(\phi)$, although the proposed method can also be used for PRC of any other quantity.

2.2. Effect of fluctuation of the period T

The period T is assumed to be a constant in Section 2.1. However, inter-spike intervals fluctuate stochastically in an experiment (Mainen & Sejnowski, 1995); this suggests that the period T itself should be considered as a random variable.

In conventional analysis, the period T in Eq. (1) is replaced by the average $\bar{T}$ of the inter-spike intervals, which corresponds to the expectation of the random variable T. The resultant estimates x_i and y_i of ϕ_i and $Z(\phi_i)$ are

$$x_i = 2\pi \frac{t_i}{\bar{T}}, \qquad y_i = 2\pi \frac{\bar{T} - T_i'}{\bar{T}}. \tag{4}$$

In most existing studies, statistical analysis, such as fitting by trigonometric or spline functions, is performed after the data are normalized by Eq. (4).

We observed that this approach does not seem optimal for our purposes. To explain the idea, we tentatively assume that we know the timing T_i of the next spike when the perturbation *does not* exist. The value T_i can be regarded as a realization of the random variable T in the ith trial. We can then define an i-dependent normalization as

$$x_i' = 2\pi \frac{t_i}{T_i}, \qquad y_i' = 2\pi \frac{T_i - T_i'}{T_i}, \tag{5}$$

which leads to different estimates (x_i', y_i') of $(\phi_i, Z(\phi_i))$. The direct use of Eq. (5) is usually impossible in the analysis of a real experiment where we cannot observe T_i. However, when we know T_i, we obtain results better than those from Eq. (4).

To confirm this, we design the following numerical experiment. When we simulate a mathematical neuron model with noise on a computer, we can generate pairs of "perturbed" and "unperturbed" time-series of spikes using the same random number sequences. For the ith pair, a perturbation is added at $t = t_i$ for only the "perturbed" series. In this case, we can regard the inter-spike interval in the ith "unperturbed" series as T_i, which cannot be measured in a real experiment. Thus, we can realize the normalization with Eq. (5) and compare it to the results using Eq. (4).

Fig. 2 shows the results of the experiment where the data is generated by the noisy Morris–Lecar equation (see Section 5.1). The values (x_i', y_i') of the variable normalized by Eq. (5) are plotted in the right panel, while the values (x_i, y_i) of the variable normalized by Eq. (4) are plotted in the left panel. The solid curve common to the panels corresponds to true PRC, estimated by numerical experiments without the noise term. The points (x_i', y_i') give a better approximation for the PRC, which supports our conjecture.

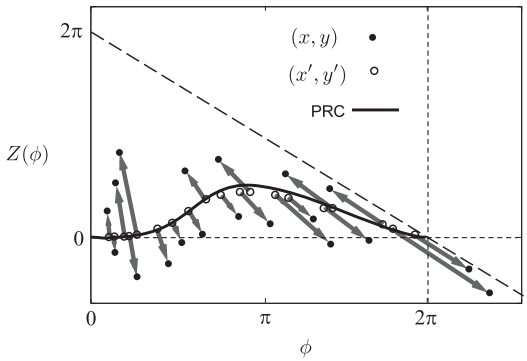

Fig. 3. Correlated errors in an estimated PRC. The arrows showing the correlation never exceed the broken line, which corresponds to the constraint $t_i \le T_i'$.

An important observation is that the fluctuation of T_i causes a correlation between x_i and y_i as defined by Eq. (4). From Eqs. (4) and (5), the difference between (x_i, y_i) and (x_i', y_i') is written as

$$\begin{aligned} x_i - x_i' &= x_i \delta_i, \\ y_i - y_i' &= (y_i - 2\pi)\delta_i, \end{aligned} \tag{6}$$

where δ_i is defined by

$$\delta_i = \frac{T_i - \bar{T}}{T_i}. \tag{7}$$

If we assume that a point $(\phi_i, Z(\phi_i))$ on the true PRC is approximated well by the improved estimate (x_i', y_i'), the difference $(x_i - x_i', y_i - y_i')$ can be regarded as the error of the naive estimate (x_i, y_i). Eq. (6) indicates that the errors in the explanatory variable are not negligible and that there is a strong correlation between the errors in the explanatory and response variables.

Fig. 3 visualizes the correlation in the data of Fig. 2. Each arrow in Fig. 3 represents the vector $(x_i - x_i', y_i - y_i')$, where the starting point of the arrow is (x_i', y_i') and the endpoint is (x_i, y_i). The solid curve is the true PRC of the Morris–Lecar equation. The correlation is shown by the systematic distribution of the lengths and directions of the arrows and is clearly seen in the data.

2.3. Estimation of unobserved T_i

In real experiments, we cannot identify T_i directly. Our strategy in this study is to estimate both $Z(\cdot)$ and $\{T_i\}$ simultaneously. Here, we give a rough sketch of the concept. The proposed method will be considered in detail in Sections 3 and 4.

In the previous section, we identified the points $\{(x'_i, y'_i)\}$ to $\{(\phi_i, Z(\phi_i))\}$, but there is actually some observational noise, i.e., we can write

$$x'_i = \phi_i + \eta_i,$$
$$y'_i = Z(\phi_i) + \varepsilon_i, \tag{8}$$

where η_i and ε_i are small residual terms. Hereafter, we set $\eta_i = 0$. Later, in the analysis detailed in Section 3, we will assume that $\{\varepsilon_i\}$ are samples from the normal distribution $\mathcal{N}(0, \sigma^2)$.

Using Eqs. (6) and (8) with $\eta_i = 0$, we have the relation

$$x_i = \phi_i + x_i\delta_i, \tag{9}$$
$$y_i = Z(\phi_i) + (y_i - 2\pi)\delta_i + \varepsilon_i. \tag{10}$$

Note that δ_i in Eqs. (9) and (10) is defined from T_i by Eq. (7), and the data (x_i, y_i) is the output of an experiment normalized by the conventional Eq. (4). Given the function $Z(\cdot)$ and a prior distribution of δ_is, we can estimate $\{\delta_i\}$ (or equivalently $\{T_i\}$) using Eqs. (9) and (10). On the other hand, given a set of $\{\delta_i\}$, Eqs. (9) and (10) are reduced to a functional regression problem of estimating $Z(\cdot)$, which can be treated by assuming some parametric form or smoothness of the function $Z(\cdot)$.

Roughly speaking, our goal of estimating both $Z(\cdot)$ and $\{\delta_i\}$ simultaneously can be attained by solving the undetermined stochastic equations Eqs. (9) and (10) with assumptions for $Z(\cdot)$ and $\{\delta_i\}$. However, formulating and solving such a complicated problem is not easy. In this study, a combination of a Bayesian framework and MCMC is proposed as a systematic solution to the problem, which will be explained in the following sections.

3. Bayesian model of phase response curves

3.1. Bayesian framework

As discussed in the previous section, our task can be summarized as a simultaneous estimation of $Z(\cdot)$ and $\{\delta_i\}$ from the data $\{(x_i, y_i)\}$ defined by Eq. (4). In a Bayesian framework, we begin with writing down the simultaneous density of relevant variables. Given δ_i, we can erase ϕ_i using the deterministic relation Eq. (9) and data $\{x_i\}$. The simultaneous density of y, Z and δ is then written as

$$p(y, Z, \delta) = p(y|Z, \delta)\, p(Z)\, p(\delta). \tag{11}$$

Our Bayesian model now consist of three components; the likelihood function $p(y|Z, \delta)$, and the prior distributions $p(Z)$ and $p(\delta)$, which will be defined in Sections 3.3–3.5. Once these components are defined, the simultaneous density Eq. (11) is explicitly given, and the Bayes theorem provides the posterior density

$$p(Z, \delta|y) = \frac{p(y|Z, \delta)\, p(Z)\, p(\delta)}{\int\int p(y|Z, \delta)\, p(Z)\, p(\delta) \mathrm{d}\delta\, \mathrm{d}Z} \tag{12}$$

of Z and δ. In the Bayesian framework, estimators of any quantity are derived from Eq. (12). For example, we can estimate the curve $Z(\cdot)$ that minimizes the posterior expectation of the mean square loss as an average of Z over the distribution defined by the density Eq. (12).

In Eq. (12), the symbols $\int \cdots \mathrm{d}\delta$ and $\int \cdots \mathrm{d}Z$ denote multiple integration and integration in a function space, respectively; the latter is approximated by finite dimensional integrals in an actual computation. Even with such an approximation, the sampling and calculation of averages with the posterior distribution Eq. (12) is far from trivial. This will be treated by MCMC in Section 4.

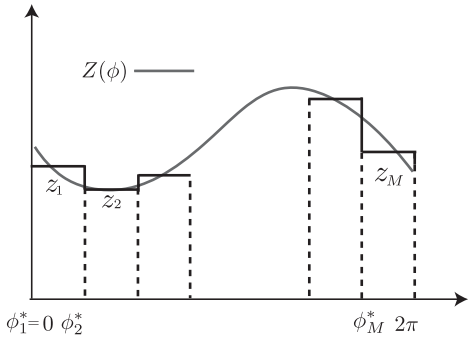

Fig. 4. Representation of the function $Z(\cdot)$.

3.2. Representation of $Z(\cdot)$

Before defining the factors on the right-hand side of Eq. (11), let us fix a representation of the function $Z(\cdot)$. We use a naive discretization of $Z(\cdot)$; this representation is convenient for our problem, where $\{x'_i\}$ are not uniformly separated and should be estimated from data.

We divide the ϕ axis into M successive intervals $\{[\phi_j^*, \phi_{j+1}^*), j = 1, \ldots, M\}$ of equal lengths. The piecewise constant curve $Z(\cdot)$ indexed with $z = (z_1, \ldots, z_M)^T$ is then defined by $Z(\phi) = z_j$ for $\phi \in [\phi_j^*, \phi_{j+1}^*)$. Here $(\ )^T$ denotes the transpose of a vector. These definitions are illustrated in Fig. 4.

When we use the discretized representation of $Z(\cdot)$ defined here, it is convenient to define the $n \times M$ matrix function $E(v)$ of $v = \{v_i\}$, whose (i, j) component is given by

$$E_{ij}(v) = \begin{cases} 1 & v_i \in [\phi_j^*, \phi_{j+1}^*) \\ 0 & v_i \notin [\phi_j^*, \phi_{j+1}^*), \end{cases} \tag{13}$$

which we will use in Section 3.3.

3.3. Likelihood $p(y|Z, \delta)$

Let us begin with Eq. (8) in Section 2.3. Assuming that $\{\varepsilon_i\}$ are independently distributed with the normal distribution $\mathcal{N}(0, \sigma^2)$, the probability density $p(y'|Z)$ of y' is written as

$$p(y'|z) = \frac{1}{\sqrt{2\pi\sigma^2}} \exp\left\{-\frac{1}{2\sigma^2}\|y' - E(x')z\|^2\right\}, \tag{14}$$

where x' and y' are defined as vectors whose ith components are given by x'_i and y'_i in Eq. (5), respectively. Here, z is the discretized representation of $Z(\cdot)$ and we use the $n \times M$ matrix $E(x')$ defined by Eq. (13).

To obtain an explicit form of the density $p(y|z, \delta)$, the stochastic variable y' in Eq. (14) should be changed to y. In addition, the variable x' should be represented by x_i and δ_i. This can be done with the following relation,

$$x'_i = (1 - \delta_i)x_i, \tag{15}$$
$$y'_i = (1 - \delta_i)y_i + 2\pi\delta_i, \tag{16}$$

which is derived from Eq. (6). Using Eq. (15), the density $p(y|z, \delta)$ can be expressed in the matrix form

$$p(y|z, \delta) = \left\{\prod_{i=1}^{n} \frac{(1 - \delta_i)}{\sqrt{2\pi\sigma^2}}\right\} \exp\left\{-\frac{1}{2\sigma^2}\|y'(\delta) - E(x'(\delta))z\|^2\right\}, \tag{17}$$

where $x'(\delta)$ and $y'(\delta)$ are defined as vectors whose ith components are given by $x'_i(\delta) = (1 - \delta_i)x_i$ and $y'_i(\delta) = (1 - \delta_i)y_i + 2\pi\delta_i$, respectively. Note that the variance of y_i is computed as $\sigma^2/(1 - \delta_i)^2$, which corresponds to the normalization factor $(1 - \delta_i)/\sqrt{2\pi\sigma^2}$ in Eq. (17).

3.4. The prior $p(\delta)$

A simple choice for the prior distribution of T_i is a normal distribution. However, it is reasonable to assume that $t_i \leq T_i$, because a neuron should fire after the perturbation is added. Thus, it is better to assume a truncated normal distribution $\mathcal{N}_{[t_i,\infty)}(\bar{T}, \sigma_T)$ as the prior distribution of T_i, whose density is given by

$$p(T_i) = \begin{cases} \dfrac{1}{\Xi_i} \exp\left\{-\dfrac{(T_i - \bar{T})^2}{2\sigma_T^2}\right\}, & t_i \leq T_i, \\ 0, & \text{otherwise.} \end{cases} \tag{18}$$

When we change the variable from T_i to $\delta_i = (T_i - \bar{T})/T_i$, it is transformed to the prior density of δ_i

$$p(\delta_i) = \begin{cases} \dfrac{1}{\Xi_i'} \dfrac{1}{(1-\delta_i)^2} \\ \quad \times \exp\left\{-\dfrac{1}{2(\sigma_T/\bar{T})^2} \dfrac{\delta_i^2}{(1-\delta_i)^2}\right\}, & 1 - \dfrac{2\pi}{x_i} \leq \delta_i < 1. \\ 0, & \text{otherwise.} \end{cases} \tag{19}$$

Here Ξ_i and Ξ_i' are the normalization constants. The prior $p(\delta)$ is expressed as $\prod_{i=1}^n p(\delta_i)$ with $p(\delta_i)$ defined by Eq. (19).

3.5. The prior $p(Z(\cdot))$

We assume that the PRCs are smooth and periodic functions. To represent this, a smoothness prior of $Z(\cdot)$ is introduced. Using the discretized representation of $Z(\cdot)$, it is expressed as

$$p(z) = \frac{1}{\Xi(d)} \exp\left\{-\frac{d^2}{2} \sum_{j=1}^{M} (z_{j-1} - 2z_j + z_{j+1})^2\right\}, \tag{20}$$

where we assume the periodic boundary condition $z_0 = z_M$, $z_{M+1} = z_1$. Eq. (20) can also be expressed in the matrix form

$$p(z) = \frac{1}{\Xi(d)} \exp\left(-\frac{d^2}{2}\|Dz\|^2\right), \tag{21}$$

where the $M \times M$ matrix D is defined by

$$D = \begin{bmatrix} -2 & 1 & 0 & \dots & 0 & 0 & 1 \\ 1 & -2 & 1 & 0 & \dots & 0 & 0 \\ 0 & 1 & -2 & 1 & \dots & 0 & 0 \\ 0 & 0 & 1 & -2 & \dots & 0 & 0 \\ \vdots & \vdots & \vdots & \ddots & \ddots & \vdots & \vdots \\ 0 & 0 & 0 & \dots & 1 & -2 & 1 \\ 1 & 0 & 0 & \dots & 0 & 1 & -2 \end{bmatrix}. \tag{22}$$

The term $(z_{j-1} - 2z_j + z_{j+1})^2$ in Eq. (20) represents the smoothness of the curve $Z(\cdot)$; when the hyperparameter d is larger, the estimated PRC $Z(\cdot)$ becomes smoother. This prior is essentially the same as the one introduced by Aonishi and Ota (2006), but here we utilize the discretized representation $\{z_j\}$ of the PRC $Z(\cdot)$ defined in Section 3.2. Smoothness priors in statistical science and machine learning have been discussed in the literature, *e.g.*, Titterington (1985), Wahba (1990), Kitagawa and Gersch (1996), MacKay (1992); regression using discretized representation and a smoothness prior is also considered to be a version of spline regression (Wahba, 1990).

Precisely speaking, Eq. (20) defines an improper prior of z, that is, we cannot give a finite normalization constant $\Xi(d)$ without some additional regularization term. However, it is harmless for our purpose of estimating z and the hyperparameters defined in Section 3.6. The latter is because we can separate a finite part of $\Xi(d)$ that reproduces the correct dependence of $\Xi(d)$ on d.

An alternative choice for the prior comes from the use of the fixed boundary condition $Z(0) = 0$, which is a consequence of the refractory period of a neuron and biologically plausible. In this case, the matrix form of the prior becomes

$$p(z) = \frac{1}{\tilde{\Xi}(d)} \exp\left(-\frac{d^2}{2}\|\tilde{D}z\|^2\right), \tag{23}$$

where $\tilde{D}$ is given by deleting the first row of the matrix D. In this case, the prior Eq. (23) is proper.

3.6. Hyperparameters

The Bayesian model defined in this section contains the tunable parameters $\sigma_T, \bar{T}, \sigma$, and d. Among these, σ_T and $\bar{T}$ can be measured in a preliminary experiment without perturbations. On the other hand, σ and d are difficult to determine from auxiliary information and should be estimated from the present data $\{(x_i, y_i)\}$. In this study, these two parameters are treated as "hyperparameters" of the model and estimated by an empirical Bayesian method (Akaike, 1980; Good, 1965; MacKay, 1992; Titterington, 1985) that maximizes the marginal likelihood

$$l(y|\sigma, d) = \int\int p_\sigma(y|z, \delta) p_d(z) p(\delta)\, \mathrm{d}\delta \mathrm{d}z \tag{24}$$

of hyperparameters σ and d. Here we explicitly show the dependence of $p(y|z, \delta)$ and $p(z)$ on the hyperparameters as $p_\sigma(y|z, \delta)$ and $p_d(z)$. Utilizing the output of MCMC for maximizing Eq. (24) will be discussed in Section 4.

4. Markov chain Monte Carlo (MCMC)

4.1. The basic algorithm

As explained in Section 3, once we define a Bayesian model, the posterior distribution $p(z, \delta|y)$ is automatically derived by Bayes' theorem. It is, however, difficult to give an analytical representation of posterior averages because our likelihood and prior are very complicated. Here, we introduce a Markov chain Monte Carlo (MCMC) algorithm that consists of alternate sampling of z and δ.

The sampling of z is defined by drawing a new value of z according to the conditional density $p(z|\delta, y)$, which is given by the normal density with the mean

$$\mu_z = (E^T E + \sigma^2 d^2 D^T D)^{-1} E^T y', \tag{25}$$

and variance

$$\Sigma_z = \left(\frac{1}{\sigma^2} E^T E + d^2 D^T D\right)^{-1}, \tag{26}$$

where E and y' are shortened forms of $E(x'(\delta))$ and $y'(\delta)$, respectively. The matrices $E(x'(\delta))$ and D and the vector function $y'(\delta)$ used here are defined in Sections 3.2, 3.3 and 3.5. Using the Cholesky decomposition of the matrix Σ_z^{-1}, all components of z are generated simultaneously by a standard method (see, for example, Gelman et al., 2003).

Sampling of δ is a little difficult because the distribution of δ conditional on z is complicated and direct sampling is impossible. Here, we use the Metropolis method, which is a version of the MCMC methods. Our implementation of the Metropolis method is as follows: first, we randomly select a component δ_i of δ. A candidate δ_i^{cand} for a new value of δ_i is then generated near the current value δ_i^{curr} of δ_i, as $\delta_i^{\mathrm{cand}} = \delta_i^{\mathrm{curr}} + \epsilon$, where $\epsilon \sim \mathcal{N}(0, \kappa^2)$

and the constant κ^2 is a parameter of the algorithm. Finally, the candidate $\delta_i^{\rm cand}$ is accepted or rejected by comparing the ratio

$$q = \frac{p(\delta_i^{\rm cand}|\delta_{-i}, z, y)}{p(\delta_i^{\rm curr}|\delta_{-i}, z, y)} \tag{27}$$

to a uniform random number $r \in [0, 1)$ that is generated independently. If $r \leq q$, the candidate $\delta_i^{\rm cand}$ is accepted as a new value of δ_i. Otherwise, if $r > q$, the candidate is rejected and we keep the current value $\delta_i = \delta_i^{\rm curr}$. Note that δ_{-i} in Eq. (27) indicates $\{\delta_j\}, j \neq i$.

Summary of the MCMC algorithm

1. Initialize z and δ. Set a counter $N_{\rm MC} = 0$.
2. Update z.
   - Compute the Cholesky decomposition of the matrix Σ_z^{-1}.
   - Draw a new value of the random number z according to the normal distribution defined by μ_z and Σ_z^{-1}.
3. Update δ.
   - Choose i randomly.
   - Draw $\epsilon \sim \mathcal{N}(0, \kappa^2)$ and define the candidate by $\delta_i^{\rm cand} = \delta_i^{\rm curr} + \epsilon$, where $\delta_i^{\rm curr}$ is the current value of δ_i.
   - Compute the ratio q by Eq. (27).
   - Draw a uniform random number $r \in [0, 1)$. Set the value of δ_i to $\delta_i^{\rm cand}$ if $r \leq q$.

   * It is possible to define a modification where this step is repeated multiple times.
4. Set $N_{\rm MC} = N_{\rm MC} + 1$. If $N_{\rm MC}$ is smaller than the prescribed value, return to step 2. Otherwise, terminate the procedure.

These steps define an ergodic Markov chain with the stationary density $p(z, \delta|y)$. By simulating the Markov chain, we can draw samples of z and δ according to the posterior density $p(z, \delta|y)$. These samples are correlated but can be used for computing posterior averages. Details of the general theory of MCMC can be found in books by Gelman et al. (2003), Gilks et al. (1995), MacKay (2003) and Robert and Casella (2004); some examples of applications of MCMC to models with errors in explanatory variables are found in Berry et al. (2002), Gilks et al. (1995) and Caroll et al. (2006).

4.2. Replica exchange Monte Carlo

The algorithm defined in the previous section is a standard example of Markov Chain Monte Carlo used in Bayesian statistics. It works if the number of iterations is sufficiently large. However, the number of iterations necessary to obtain stable results using such an algorithm can be very large in a complicated problem, which is known as "slow mixing" or "slow relaxation". We found that our problem of estimating PRCs from data with correlated errors is a typical example of slow mixing. In a range of hyperparameters, we can barely get stable results using a naive MCMC algorithm.

To deal with this difficulty, we introduce the replica exchange Monte Carlo algorithm (REM), which is also known as parallel tempering or Metropolis coupled MCMC (Geyer, 1991; Hukushima & Nemoto, 1996; Iba, 2001).

The REM is designed to increase the efficiency of MCMC by connecting a fast mixing "easy" region to the slow mixing "difficult" region. The REM shares this idea with the simulated annealing algorithm for optimization, but there is an important difference. While simulated annealing is designed for obtaining an optimal solution and does not necessarily reproduce correct averages of statistics with a given distribution, the REM is designed for correct sampling and calculation of averages.

To implement the REM, we prepare N copies of the systems (replicas), each of which corresponds to the density $p(\omega_k|\gamma_k)$ parameterized by γ_k. Hereafter the state of the kth replica is represented by ω_k. We also assume that $\gamma_1 < \gamma_2 < \cdots < \gamma_N$, where

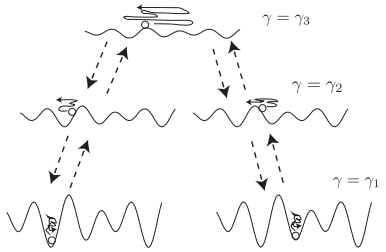

Fig. 5. Schematic view of replica exchange Monte Carlo. For each value γ_k of γ, the landscape sampled by MCMC is shown by the curve that represents $-\log p(\cdot|\gamma_k)$. A case for three replicas is shown in the figure, while 32 replicas are used in examples in the text.

parameters γ_1 and γ_N correspond to the parameters where the slowest and fastest mixing are observed, respectively. The idea of the REM is to introduce occasional swaps of the states ω_k and ω_{k+1} of the replicas with the neighboring parameters γ_k and γ_{k+1}. The swap is performed as follows.

- Choose the index k of a replica randomly.
- Calculate the ratio

$$\tilde{q} = \frac{p(\omega_{k+1}|\gamma_k)p(\omega_k|\gamma_{k+1})}{p(\omega_k|\gamma_k)p(\omega_{k+1}|\gamma_{k+1})}. \tag{28}$$

- Draw a uniform random number $r \in (0, 1]$ and swap the pair if $r < \tilde{q}$.

The entire REM algorithm consists of a basic MCMC algorithm applied to each replica and the swap of replicas defined as above.

An essential property of the swapping procedure of the REM is that it is designed to make the simultaneous density

$$p(\omega_1, \ldots, \omega_N) = \prod_{k=1}^{N} p(\omega_k|\gamma_k) \tag{29}$$

stationary. Through the swapping procedure, the states of the replicas in the fast mixing region propagate to the slow mixing region, which realizes an annealing effect as shown in Fig. 5. Even with such a state propagation, we can reproduce the correct averages at all values $\{\gamma_k\}$ of the parameter γ, because the simultaneous density Eq. (29) represents the stationary distribution of the REM.

So far, we have discussed a generic algorithm. When the REM is used in statistical physics, the parameter γ in the generic algorithm usually corresponds to the temperature of a system. How can we choose the parameter γ in the present example of posterior sampling?

A basic observation is that, as the values of hyperparameters σ^2 and $1/d^2$ become larger, the variance of the posterior also becomes larger. Keeping this in mind, we transform the set (σ, d) of hyperparameters to (α, β) with

$$\alpha = \sigma d, \qquad \beta = \sigma/d. \tag{30}$$

Here, the hyperparameter β corresponds to the temperature in statistical physics. In a Gaussian model where the errors in the explanatory variable are ignored (Aonishi & Ota, 2006; Ota et al., 2009), α determines the shape of the estimated curve while β determines the variance around the curve. However, in the proposed model, both hyperparameters affect the estimated PRC.

Then, the hyperparameter β is the natural choice for the role of γ; the density $p(\omega_k|\gamma_k)$ in the generic algorithm is replaced with $p(z, \delta|y, \beta_k)$, which defines the REM for the proposed model.

To design an efficient REM, the variance κ^2 of the proposal distribution used in the basic algorithm should depend on the index k of replicas. In Section 5, we use the following formula:

$$\kappa_k = \frac{\kappa_N - \kappa_1}{N - 1} \times (k - 1) + \kappa_1, \tag{31}$$

for the value κ_k of κ in the kth replica. This formula gives a larger value of κ when β is large. The constants κ_1 and κ_N are determined to keep the acceptance ratios in the basic algorithm within a reasonable range, which is usually around ∼50%.

Using the REM with these remarks, the mixing of MCMC for large or medium values of α become fast enough for the practical use of the proposed method. However, it is still difficult to treat the problem with a smaller value of α, where MCMC does not mix well. Here, we employ the following trick that realizes a kind of annealing by decreasing α: first we run MCMC with the largest value of α, using a REM that consists of parallel runs with different values of β. Then, we decrease the value of α sequentially using the same set of β, where each run of MCMC is initialized by a sample from the previous run with a larger α.

Although an artificial choice of initial conditions in this scheme is not fully justified from the spirit of MCMC, this method gives reasonable results in the following sections and is considered to be a practical approach to the problem. A better founded solution may be obtained with some improved version of the REM, which is left for future studies.

4.3. Estimation of hyperparameters

Here, we explain how to utilize the MCMC output to estimate hyperparameters. In an empirical Bayes procedure, hyperparameters are estimated through a maximization of the marginal likelihood Eq. (24). The marginal likelihood cannot be directly computed with samples from the posterior distribution $p(z, \delta|y)$. Log-derivatives of the marginal likelihood by hyperparameters, however, can be computed using MCMC, which is usually sufficient for searching hyperparameters that maximize the marginal likelihood.

Taking the log-derivatives of Eq. (24), we obtain

$$\frac{\partial \log l(y|\sigma, d)}{\partial (d^2)} = -\frac{1}{2}\mathbb{E}_{\mathrm{pos}}\left[\|Dz\|^2\right] + \frac{M}{2d^2}, \tag{32}$$

$$\frac{\partial \log l(y|\sigma, d)}{\partial (1/\sigma^2)} = -\frac{1}{2}\mathbb{E}_{\mathrm{pos}}\left[\,\|y'(\delta) - E(x'(\delta))z\,\|^2\right] + \frac{n\sigma^2}{2}, \tag{33}$$

where $\mathbb{E}_{\mathrm{pos}}[f]$ denotes the posterior average of a function f of z and δ as

$$\mathbb{E}_{\mathrm{pos}}[f] = \int\int f(z, \delta)p(z, \delta|y)\,\mathrm{d}z\mathrm{d}\delta. \tag{34}$$

Thus, computing the log-derivatives of the marginal likelihood is reduced to calculating the posterior averages, which can be treated by MCMC.

As discussed in the previous section, it is natural to use the hyperparameters α and β defined by Eq. (30), instead of σ and d. To maximize the marginal likelihood with respect to α and β, we can use the relations

$$\frac{\partial \log l(y|\sigma, d)}{\partial \alpha} = \frac{1}{\beta}\frac{\partial \log l(y|\sigma, d)}{\partial (d^2)} - \frac{1}{\alpha^2\beta}\frac{\partial \log l(y|\sigma, d)}{\partial (1/\sigma^2)}, \tag{35}$$

$$\frac{\partial \log l(y|\sigma, d)}{\partial \beta} = -\frac{\alpha}{\beta^2}\frac{\partial \log l(y|\sigma, d)}{\partial (d^2)} - \frac{1}{\alpha\beta^2}\frac{\partial \log l(y|\sigma, d)}{\partial (1/\sigma^2)}. \tag{36}$$

An example of hyperparameter estimation using Eq. (32)–(36) will be shown in Section 5.2.

5. Numerical experiments with artificial data

5.1. The Morris–Lecar equation

In this section, we test the proposed method with artificial data generated by a neuron model. Here we employ the noisy Morris–Lecar equation (Morris & Lecar, 1981) as a source of artificial data; this is a bivariate stochastic differential equation widely used in neural science. This neuron model is defined by a set of equations:

$$\begin{aligned}\frac{\mathrm{d}V}{\mathrm{d}t} &= -g_{\mathrm{Ca}}M_\infty(V)(V - V_{\mathrm{Ca}}) - g_{\mathrm{K}}N(V - V_{\mathrm{K}}) \\ &\quad - g_{\mathrm{leak}}(V - V_{\mathrm{leak}}) + \xi(t) + I(t), \\ \frac{\mathrm{d}N}{\mathrm{d}t} &= \frac{N_\infty(V) - N}{\tau_N(V)},\end{aligned} \tag{37}$$

where the variables V and N represent the voltage of the neuron and the ratio of open K^+ channels, respectively. The functions $M_\infty(V)$, $N_\infty(V)$ and $\tau_N(V)$ are defined by

$$\begin{aligned}M_\infty(V) &= \frac{1 + \tanh\{(V - V_1)/V_2\}}{2}, \\ N_\infty(V) &= \frac{1 + \tanh\{(V - V_3)/V_4\}}{2}, \\ \tau_N(V) &= \frac{1}{\cosh\{(V - V_3)/(2V_4)\}}.\end{aligned} \tag{38}$$

The values of parameters used in this study are as follows: $g_{\mathrm{Ca}} = 1.1$, $g_{\mathrm{K}} = 2.0$, $g_{\mathrm{leak}} = 0.5$, $V_{\mathrm{Ca}} = 100$, $V_{\mathrm{K}} = -70$, $V_{\mathrm{leak}} = -50$, $V_1 = -1.0$, $V_2 = 15.0$, $V_3 = 10.0$, and $V_4 = 14.5$.

The term $\xi(t)$ represents white noise added to the voltage component, which satisfies the relations

$$\mathbb{E}[\xi(t)] = 0, \qquad \mathbb{E}[\xi(t)\xi(t')] = s^2\delta(t - t'), \tag{39}$$

where δ denotes Dirac's δ-function. The current $I(t)$, which comes from the outside of a neuron, is assumed to be given by

$$I(t) = I_c + I_p\delta(t - t_i), \tag{40}$$

where the values of I_c and I_p are 8 and 2, respectively.

To solve the stochastic differential equation and generate artificial data, we use the Euler–Maruyama method (Kloeden & Platen, 2000). The "true" PRCs shown in the following section are calculated by a linear interpolation of points given by simulations of the noiseless Morris–Lecar equation ($s = 0$).

5.2. Example

Here, we show an example of the estimation of PRC from a set of artificial data through the proposed method. The result of the proposed method is compared with the true PRC estimated with noiseless experiments.

The result of the proposed method is also compared with the result of conventional Bayesian regression with a smoothness prior, where the errors in the explanatory variable are ignored. This algorithm employs the same representation and smoothness prior of $Z(\cdot)$, but assumes that

$$y_i = Z(x_i) + \varepsilon_i, \quad \varepsilon_i \sim \mathcal{N}(0, \sigma^2). \tag{41}$$

It is similar to that proposed by Aonishi and Ota (2006) and Ota et al. (2009). Hereafter, we call this algorithm the "conventional spline", because, as mentioned earlier, it is considered to be a version of spline regression; the term "conventional" indicates that it does not contain errors in the explanatory variable.

To apply the conventional spline, the value x_i of the explanatory variable should satisfy the relation $x_i < 2\pi$. This means that we should discard samples with $x_i \geq 2\pi$ when we apply the conventional spline. In the following experiments using artificial data, we remove such samples from the input of the conventional spline. To keep the number of samples and make the comparison fair, an equal number of new samples satisfying $x_i < 2\pi$ are generated and added to the input data.

The set of artificial data used here contains $n = 100$ samples, where the timing of the perturbation $\{t_i\}_{i=1}^n$ is randomly chosen.

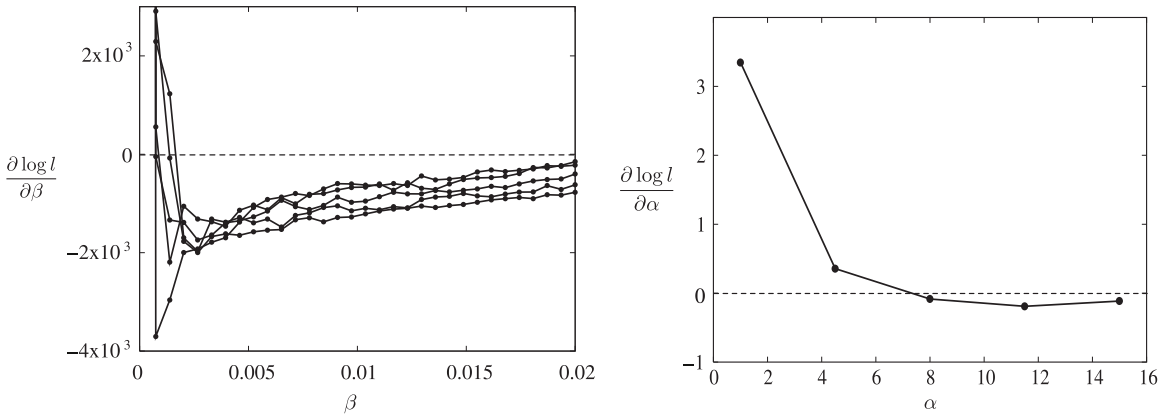

Fig. 6. Log derivatives of the marginal likelihood with respect to hyperparameters α and β. The details are explained in the text. The five curves in the left panel correspond to $\alpha = 1$, 4.5, 8, 11.5, and 15.

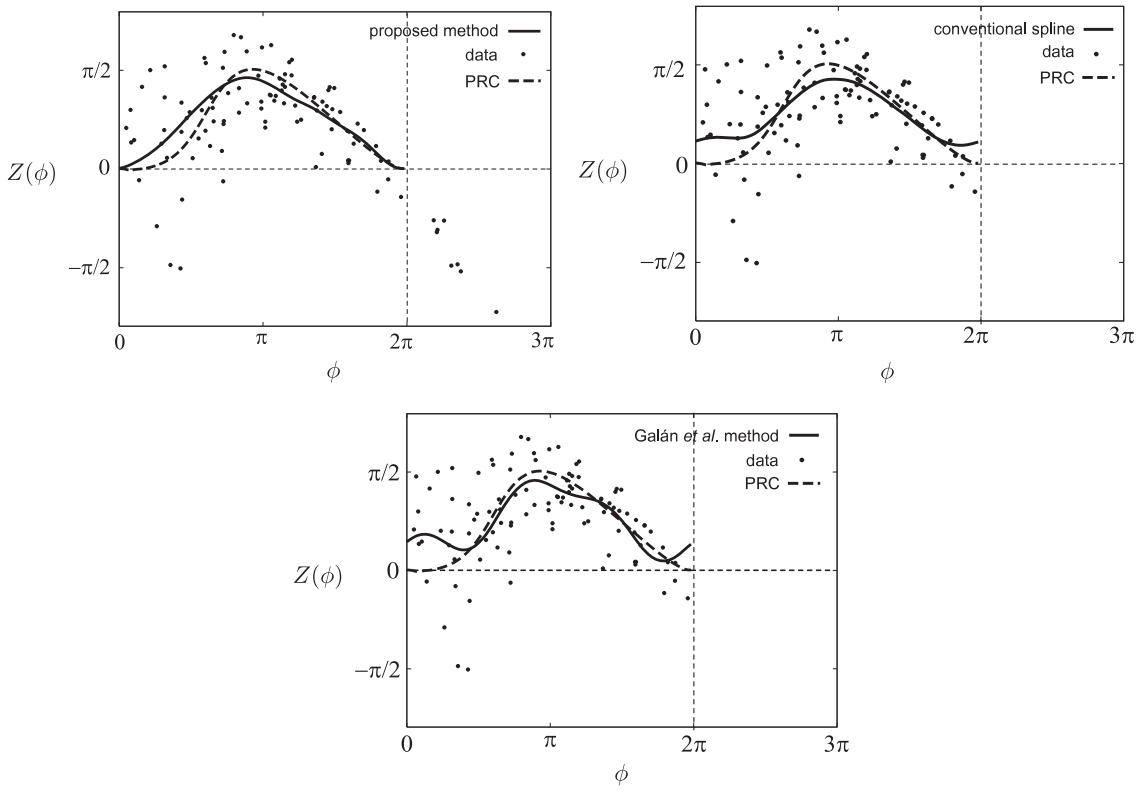

Fig. 7. Comparison between the proposed method and conventional methods using artificial data. The solid curve corresponds to the PRC estimated from samples (shown by black dots), and the broken curve shows the true PRC estimated with noiseless simulation. The upper left and upper right panels correspond to the proposed method and conventional spline, respectively; the result with the Galán et al. method is also shown in the lower panel. Differences in the samples shown in the upper left and upper right (or lower) panels are explained in the text.

The level s of the noise is 0.3. The estimates for $\bar{T}$ and σ_T are 44.2 and 6.4, respectively; these are estimated with a noiseless simulation of the same parameters.

Let us start with an estimation of the hyperparameters α and β. First, the log-derivative Eq. (36) of the marginal likelihood with respect to β is plotted with a set of values of β, as shown in the left panel of Fig. 6. Each curve corresponds to a value of α in a given set $\{\alpha_l\}$. Then, we estimate the zero crossing of each curve, which we denote as $\beta^*(\alpha_l)$. Next, for each value of $\beta^*(\alpha_l)$, we plot the log-derivative Eq. (35) of the marginal likelihood with respect to α for the values of $\alpha \in \{\alpha_l\}$, as shown in the right panel of Fig. 6. The zero crossing of this curve gives the estimate $\hat{\alpha}$ of α. The estimate $\hat{\beta}$ of β is also obtained as $\beta^*(\hat{\alpha})$. In our example, the zero crossing of the curve in Fig. 6 is located near $\alpha = 7$, and we choose $\hat{\alpha} = 8$ as a rough estimate of α from among the five values we tested here. The value of β is estimated as $\hat{\beta} = \beta^*(8) \simeq 0.00074$.

In this procedure, we assume that the zero point is unique. It is possible to introduce more sophisticated iterative procedures to find zeros; a rough estimate of α and β is usually sufficient for estimating the PRC $Z(\cdot)$.

The upper left panel of Fig. 7 shows the PRC estimated with the proposed method using the hyperparameters $\hat{\alpha}$ and $\hat{\beta}$ as defined above. For comparison, the upper right panel of Fig. 7 shows the PRC estimated with the conventional spline. The hyperparameters of the conventional spline are also determined by maximizing the corresponding marginal likelihood, where σ^2 is analytically optimized and $\hat{\alpha} = 40$ is found by a grid search. The result from using the Galán et al. method (Galán et al., 2005) is also shown in

Table 1
$\bar{T}$ and σ_T from artificial data.

s	$\bar{T}$	σ_T	$\sigma_T/\bar{T}$
0.1	45.3	2.3	0.05
0.15	44.9	3.6	0.07
0.2	45.0	4.8	0.11
0.25	44.6	5.4	0.12
0.3	44.2	6.4	0.15
0.35	44.2	7.5	0.17
0.4	43.7	7.8	0.18

the lower panel; the dataset used in the Galán et al. method is the same as that used in the conventional spline.

In each panel of Fig. 7, a solid curve shows the estimate, while a broken curve shows the true PRC. The solid curve is closer to the broken curve in the upper left panels than the one in the upper right panel, which suggests that the proposed method outperforms the conventional spline for this dataset. The proposed method is also better than the Galán et al. method in this example.

The details of the algorithm used in computing the above result are as follows. The number M of the pieces of the discretized curve $Z(\cdot)$ is 100 and the periodic boundary condition is assumed. The number of replicas N used in the REM is 32, and the number N_{MC} of iterations per replica is 10^6. We try to exchange neighboring pairs of replicas once within 20 iterations. The variance κ_k of the proposal distribution in the kth replica is defined by Eq. (31), where $\kappa_1 = 0.01$ and $\kappa_N = 0.07$; this is independent of α.

We make use of the advantage of the REM in parallel computation. Computational time on 32 cores(16 CPU) of AMD Opteron 252(2.6 GHz) is about 6 h for each dataset ($N = 100$), including the hyperparameter search on a 5×32 grid on the (α, β) plane; it reduces to about 1/3 on faster hardware with 32 cores(4 CPU) of Intel Xeon X5570(2.93 GHz). Intel C++ compiler, MPI, and LAPACK are used for the computation. For each data set, the Galán et al. method and conventional spline (including hyperparameter search) takes 2.4×10^{-5} and 1.5 s, respectively, on a core of Intel Xeon X5570(2.93 GHz) using our implementation with C++.

5.3. Root mean square error

In Section 5.2, we apply the proposed method to a set of artificial data. Here, we consider sets of simulation data and compare the proposed method with the conventional spline using a root mean square error (RMSE) defined by

$$\mathrm{RMSE} = \sum_{\nu=1}^{N_D} \left(\int_0^{2\pi} (Z(\phi) - Z^{[\nu]}(\phi))^2 \mathrm{d}\phi \right)^{1/2}, \tag{42}$$

where the number of datasets is N_D and the curve estimated from the νth dataset is denoted by $Z^{[\nu]}(\phi)$.

We consider four datasets with different levels of external noise: $s = 0.1, 0.15, 0.2, 0.25, 0.3, 0.35$, and 0.4. For each value of s, we consider the average over $N_D = 20$ sets of artificial data for the proposed method, and $N_D = 200$ sets of artificial data for the conventional spline and the Galán et al. method. Each set is generated by a simulation with a different random number sequence. The estimates of $\bar{T}$ and σ_T are shown in Table 1 with the noise level s.

The hyperparameters α and β are estimated from each dataset by the method explained in the previous sections. The parameters used for the method are the same as those defined in the previous subsection, except that the estimated value of α is considerably larger at $s = 0.35, 0.4$ and a search in a larger hyperparameter space is required.

Fig. 8 shows RMSEs for the proposed method (solid curve), for the conventional spline (broken curve), and for the Galán et al. method (chain curve); the horizontal axis corresponds to the normalized standard error $\sigma_T/\bar{T}$, which gives a measure of the fluctuation of inter-spike intervals. The figure shows that the proposed method produces better results in the region $0.15 \leq \sigma_T/\bar{T}$.

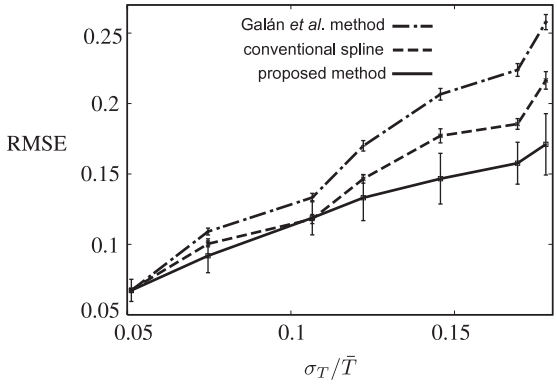

Fig. 8. Comparison of RMSE.

Table 2
$\bar{T}$ and σ_T from experimental data.

Dataset	n	$\bar{T}$ (ms)	σ_T (ms)	$\sigma_T/\bar{T}$
A	435	34.9	2.8	0.08
B	440	64.3	9.4	0.15

6. Analysis of experimental data

Finally, we test the method with experimental data recorded from the pyramidal cells in the rat motor cortex. Two datasets, A and B, are obtained using whole-cell patch-clamp recordings at the somata of layer-5 pyramidal neurons in the rat motor cortex. Details of the experiments are found in the paper Tsubo et al. (2007). The parameters $\bar{T}$ and σ_T estimated from the experimental data are shown in Table 2 as well as the number n of samples.

We use parameters for the algorithm that are essentially the same as those used in Section 5.2. In this analysis of experimental data, however, we add the condition $Z(0) = 0$ and use the prior Eq. (23) instead of Eq. (21), for both the proposed method and the conventional spline. Unlike the case of artificial data, the points $x_i \geq 2\pi$ are merely removed when the conventional spline or the Galán et al. method is applied.

The hyperparameters α and β are estimated in the same manner as that explained in Section 5.2. In the left panels of Fig. 9, the log-derivative Eq. (36) of the marginal likelihood with respect to β is plotted with the values of β. Each curve corresponds to a value of α. The zero crossing $\hat{\beta}$ is almost independent of α in the range of $1 \leq \alpha \leq 15$ in both datasets. Fixing the value of β to $\hat{\beta}$, we then plot the log-derivative Eq. (35) of the marginal likelihood with respect to α as shown in the right panels of Fig. 9. The resultant estimates of hyperparameters are $\hat{\alpha} = 4.5$ and $\hat{\beta} = 0.00058$ for dataset A and $\hat{\alpha} = 4.5$ and $\hat{\beta} = 0.00074$ for dataset B. The hyperparameters of the conventional spline are also estimated by maximizing the marginal likelihood.

The PRCs estimated with these hyperparameters are shown in Fig. 10. The left and right panels of Fig. 10 correspond to datasets A and B, respectively. In each panel, the solid curve shows the PRC estimated with the proposed method, and the broken curve shows the PRC estimated with conventional spline or the Galán et al. method. Samples in the datasets are shown by black dots. Computational time on 32 cores(16 CPU) of AMD Opteron 252(2.6 GHz) is about 49 h for each dataset ($N = 435$), including the hyperparameter search on the (α, β) plane. For the same

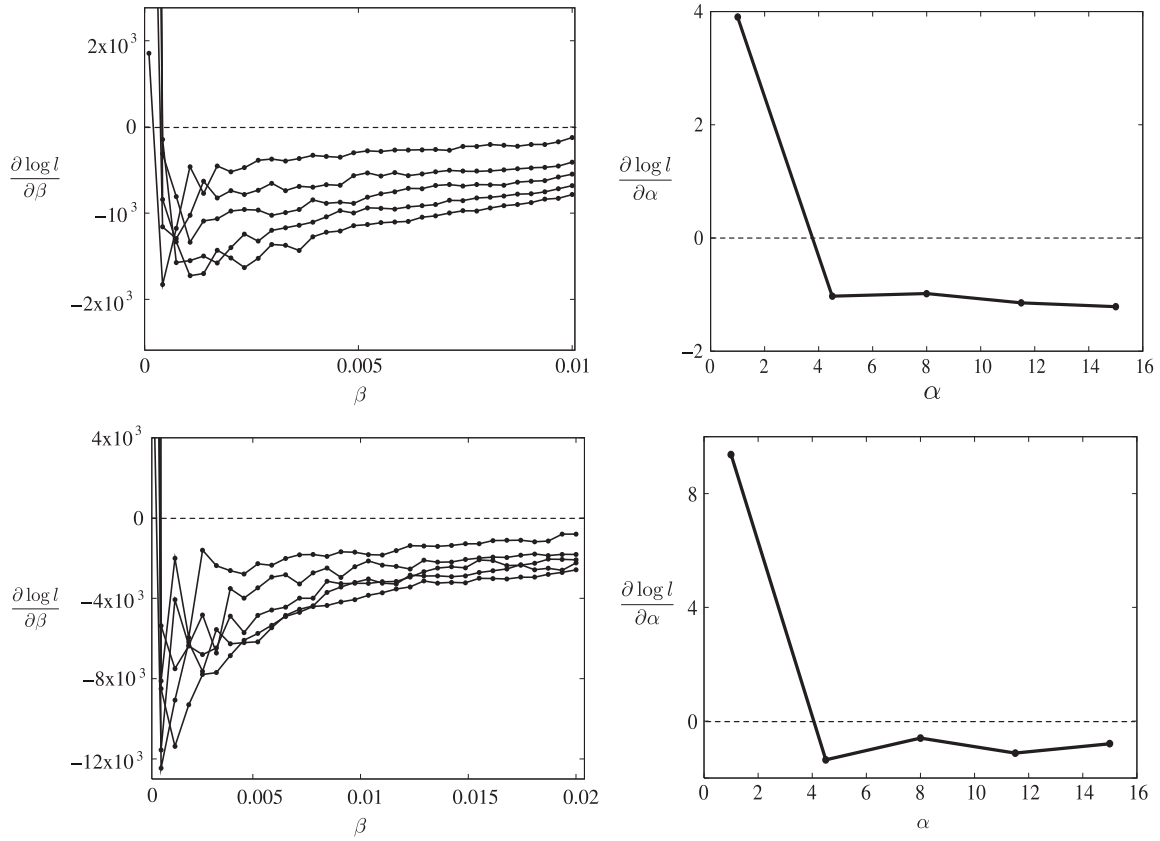

Fig. 9. Log derivatives of the marginal likelihood with respect to hyperparameters α and β (experimental data). The details are explained in the text. The five curves in the left panel correspond to $\alpha = 1$, 4.5, 8, 11.5, and 15. The upper and lower panels correspond to datasets A and B, respectively.

datasets, the Galán et al. method and conventional spline (including the hyperparameter search) take 1.3–1.7 $\times 10^{-3}$ and 3.8–3.9 s, respectively, on a core of Intel Xeon X5570(2.93GHz) using our implementation with C++.

The results shown in the left panels of Fig. 10 indicate that there is no significant improvement in using the proposed method for dataset A, where the value of $\sigma_T/\bar{T}$ is small. On the other hand, in the right panels, where the value of $\sigma_T/\bar{T}$ is larger, considerable differences are observed. This result implies the utility of the proposed method when the normalized variance $\sigma_T/\bar{T}$ is large.

7. Summary and discussion

A statistical method is introduced for estimating the PRC of a neuron. The novelty of the method is that it takes into account the correlation between errors in the explanatory and response variables of the PRC. The method is formulated in a Bayesian framework with a smoothness prior and implemented using the replica exchange Monte Carlo (REM) method, which enables efficient sampling from multimodal posterior distributions. We tested the proposed method both with artificial data generated by a neuron model and real experimental data recorded from the pyramidal cells in the rat motor cortex. The test with artificial data shows that the proposed method is advantageous when the level of noise is high. In the analysis of real experimental data with large fluctuations of spike intervals, there is a considerable difference compared to the conventional spline, which only allows for the errors in the response variable.

Although the use of the REM considerably reduces computational time, the proposed method is still highly computationally intensive. It contrasts with conventional methods such as Galán et al. (2005), which can compute estimates immediately on current hardware. More effort will be required to make our method affordable for everyday use in the laboratory. Several approaches are possible for reducing computational demands. First, we can simplify the curve representation. In this study, we use piecewise constant curves and a smoothness prior to represent PRCs; this enables flexible representation of curves with arbitrary shapes. The essential idea presented in this paper, however, can also be used with any parametric representation of PRCs, such as a linear combination of trigonometric functions; this can lead to faster algorithms. Such algorithms will be easier to use in a wet laboratory and convenient for the theoretical purpose of joining outputs from an experiment to neuron models. The second approach is to introduce a transformation that mixes explanatory and response variables, which effectively removes the correlation; then we consider regression for the transformed variable. We are currently developing research in these directions and the results will be reported elsewhere.

Recently, methods for estimating PRCs using a different type of experiment have been proposed (Ermentrout et al., 2007; Ota et al., 2009), where white or correlated noise is injected to a neuron, instead of a pulse. These experiments can be alternatives to the conventional experiments supposed in this study, although there are applications that would be difficult to treat with this approach, *e.g.,* circadian rhythm. Hence, an extension of our approach for dealing with data from these experiments will be useful. It also seems interesting to test the methods (Ermentrout et al., 2007; Ota et al., 2009) in cases with strong correlations in errors in the explanatory and response variables.

In Section 2.2, we introduced the "fluctuation of period" hypothesis as a purely phenomenological hypothesis, which is later practically justified by successful data analysis in Section 5. In the future, it is desirable to study the correlation between noise in explanatory and response variables through some theoretical analysis; such a study will elucidate the origin of the fluctuation of

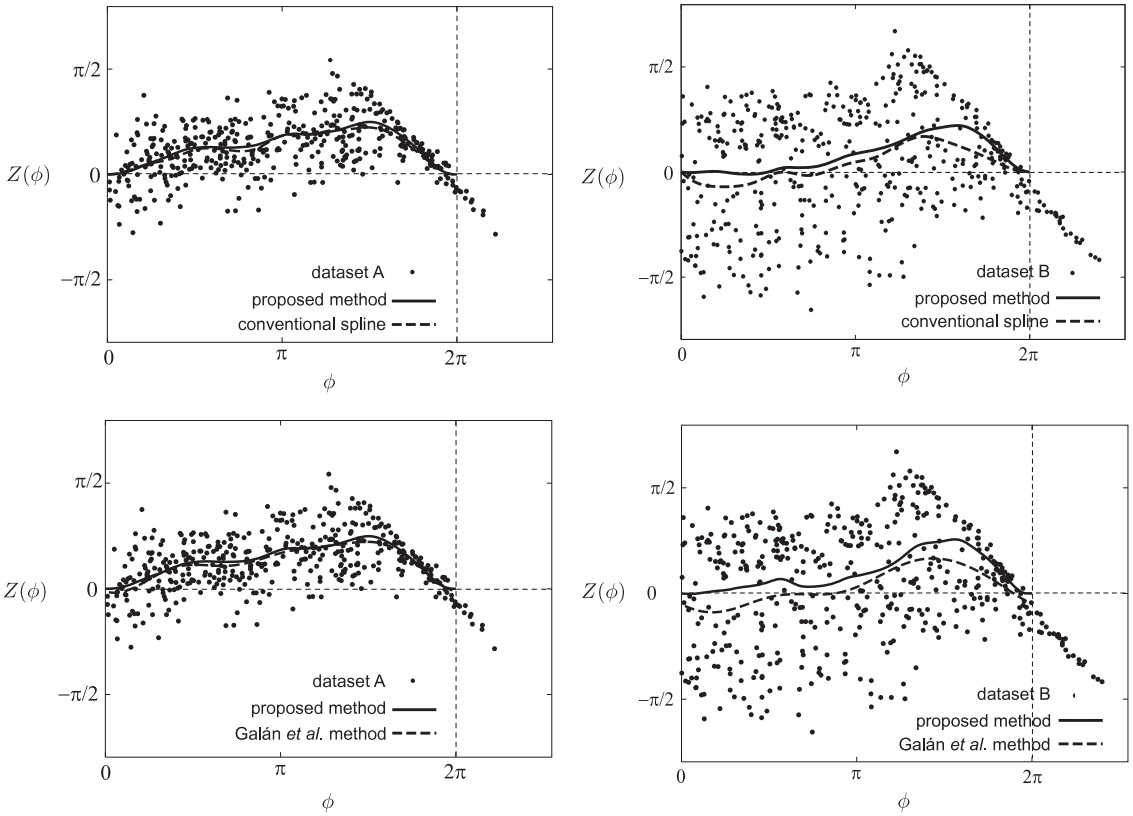

Fig. 10. Comparison between the proposed method and conventional methods using experimental data. The upper panels show a comparison to the conventional spline, while the lower panels show a comparison to the Galán et al. method. The left and right panels correspond to datasets A and B, respectively. In each panel, the solid curve shows the result of the proposed method and the broken curve shows the result of a conventional method; both are almost overlapped in the left panels. The black dots are samples.

period, and/or replace it with a different mechanism that effectively generates a similar correlation of errors. Such considerations may lead to a more realistic error model and better algorithms based on the model.

Acknowledgements

This research was supported by an allocation of computing resources of HP XC4000 and Fujitsu PRIMERGY RX200S5 from the Institute of Statistical Mathematics.

References

Acebrón, J. A., Bonilla, L. L., Pérez Vicente, C. J., Ritort, F., & Spigler, R. (2005). The Kuramoto model: A simple paradigm for synchronization phenomena. *Reviews of Modern Physics*, *77*(1), 137–185.

Akaike, H. (1980). Likelihood and the Bayesian procedure. In J. M. Bernardo, M. H. Degroot, D. V. Lindley, & A. F. M. Smith (Eds.), *Bayesian statistics* (pp. 141–166). University Press.

Amari, S., & Kawanabe, M. (1997). Information geometry of estimating functions in semi-parametric statistical models. *Bernoulli*, *3*(1), 29–54.

Aonishi, T., & Ota, Ke. (2006). Statistical estimation algorithm for phase response curves. *Journal of the Physical Society of Japan*, *75*(11), 114802.

Berry, S. M., Carroll, R. J., & Ruppert, D. (2002). Bayesian smoothing and regression splines for measurement error problems. *Journal of the American Statistical Association*, *97*(457), 160–169.

Caroll, R. J., Ruppert, D., Stefanski, L. A., & Crainiceanu, C. M. (2006). *Measurement error in nonlinear models: a modern perspective* (2nd ed.). Chapman & Hall/CRC.

Cheng, C., & Ness, J. W. V. (1999). *Statistical regression with measurement error*. Wiley.

Ermentrout, G. B. (1996). Type I membranes, phase resetting curves, and synchrony. *Neural Computation*, *8*(5), 979–1001.

Ermentrout, G. B., Galán, R. F., & Urban, N. N. (2007). Relating neural dynamics to neural coding. *Physical Review Letters*, *99*(24), 248103.

Ermentrout, G. B., & Saunders, D. (2006). Phase resetting and coupling of noisy neural oscillators. *Journal of Computational Neuroscience*, *20*(2), 179–190.

Fries, P. (2005). A mechanism for cognitive dynamics: neuronal communication through neuronal coherence. *Trends in Cognitive Sciences*, *9*(10), 474–480.

Fuller, W. A. (1987). *Measurement error models*. Wiley.

Galán, R. F., Ermentrout, G. B., & Urban, N. N. (2005). Efficient estimation of phase-resetting curves in real neurons and its significance for neural-network modeling. *Physical Review Letters*, *94*(15), 158101.

Gelman, A., Carlin, J. B., Stern, H. S., & Rubin, D. B. (Eds.). (2003). *Bayesian data analysis* (2nd ed.). Chapman & Hall/CRC.

Geyer, C. J., & Thompson, E. A. (1995). Annealing Markov chain Monte Carlo with applications to ancestral inference. *Journal of the American Statistical Association*, *90*(431), 909–920.

Geyer, C. J. (1991). Markov chain Monte Carlo maximum likelihood.. In E. M. Keramidas (Ed.)., *Computing science and statistics: Proceedings of 23rd Symposium on the Interface* (pp. 156–163). Interface Foundation.

Gilks, W. R., Richardson, S., & Spiegelhalter, D. J. (Eds.). (1995). *Markov chain Monte Carlo in practice*. Chapman & Hall.

Goldberg, J. A., Deister, C. A., & Wilson, C. J. (2007). Response properties and synchronization of rhythmically firing dendritic neurons. *Journal of Neurophysiology*, *97*(1), 208–219.

Good, I. J. (1965). *The estimation of probabilities: an essay on modern Bayesian methods*. The MIT Press.

Gray, C. M., & Singer, W. (1989). Stimulus-specific neuronal oscillations in orientation columns of cat visual cortex. *Proceedings of the National Academy of Sciences*, *86*(5), 1698–1702.

Gutkin, B. S., Ermentrout, G. B., & Reyes, A. D. (2005). Phase-response curves give the responses of neurons to transient inputs. *Journal of Neurophysiology*, *94*(2), 1623–1635.

Hansel, D., Mato, G., & Meunier, C. (1995). Synchrony in excitatory neural networks. *Neural Computation*, *7*(2), 307–337.

Huelsenbeck, J. P., & Ronquist, F. (2001). MRBAYES: Bayesian inference of phylogenetic trees. *Bioinformatics*, *17*(8), 754–755.

Hukushima, K., & Nemoto, K. (1996). Exchange Monte Carlo method and application to spin glass simulations. *Journal of the Physical Society of Japan*, *65*(6), 1604–1608.

Iba, Y. (2001). Extended ensemble Monte Carlo. *International Journal of Modern Physics C*, *12*(5), 623–656.

Izhikevich, E. M. (2007). *Dynamical systems in neuroscience: the geometry of excitability and bursting*. The MIT Press.

Jasra, A., Stephens, D. A., & Holmes, C. C. (2007). On population-based simulation for static inference. *Statistics and Computing*, *17*(3), 263–279.

Kitagawa, G., & Gersch, W. (1996). *Smoothness priors analysis of time series*. Springer.

Kloeden, P. E., & Platen, E. (2000). *Numerical solution of stochastic differential equations* (3rd ed.). Springer.

Kopell, N., & Ermentrout, G. B. (1990). Phase transitions and other phenomena in chains of coupled oscillators. *SIAM Journal on Applied Mathematics*, *50*(4), 1014–1052.
Kuramoto, Y. (1984). *Chemical oscillations, waves, and turbulence*. Springer.
MacKay, D. J. C. (1992). Bayesian interpolation. *Neural Computation*, *4*(3), 415–447.
MacKay, D. J. C. (2003). *Information theory, inference and learning algorithms*.. Cambridge University Press.
Mainen, Z. F., & Sejnowski, T. J. (1995). Reliability of spike timing in neocortical neurons. *Science*, *268*(5216), 1503–1506.
Morris, C., & Lecar, H. (1981). Voltage oscillations in the barnacle giant muscle fiber. *Biophysical Journal*, *35*(1), 193–213.
Netoff, T. I., Banks, M. I., Dorval, A. D., Acker, C. D., Haas, J. S., Kopell, N., & White, J. A. (2005). Synchronization in hybrid neuronal networks of the hippocampal formation. *Journal of Neurophysiology*, *93*(3), 1197–1208.
Ota, Ka., Nomura, M., & Aoyagi, T. (2009). Weighted spike-triggered average of a fluctuating stimulus yielding the phase response curve. *Physical Review Letters*, *103*(2), 024101.
Ota, Ke., Omori, T., & Aonishi, T. (2009). MAP estimation algorithm for phase response curves based on analysis of the observation process. *Journal of Computational Neuroscience*, *26*(2), 185–202.
Preyer, A. J., & Butera, R. J. (2005). Neuronal oscillators in aplysia californica that demonstrate weak coupling in vitro. *Physical Review Letters*, *95*(13), 138103.
Robert, C. P., & Casella, G. (2004). *Monte Carlo statistical methods* (2nd ed.). Springer.
Salinas, E., & Sejnowski, T. J. (2001). Correlated neuronal activity and the flow of neural information. *Nature Reviews Neuroscience*, *2*(8), 539–550.
Strogatz, S. H. (2000). From Kuramoto to Crawford: exploring the onset of synchronization in populations of coupled oscillators. *Physica D: Nonlinear Phenomena*, *143*(1), 1–20.
Titterington, D. M. (1985). Common structure of smoothing techniques in statistics. *International Statistical Review/Revue Internationale de Statistique*, *53*(2), 141–170.
Tsubo, Y., Takada, M., Reyes, A. D., & Fukai, T. (2007). Layer and frequency dependencies of phase response properties of pyramidal neurons in rat motor cortex. *European Journal of Neuroscience*, *25*(11), 3429–3441.
Varela, F., Lachaux, J. P., Rodriguez, E., & Martinerie, J. (2001). The brainweb: Phase synchronization and large-scale integration. *Nature Reviews Neuroscience*, *2*(4), 229–239.
Wahba, G. (1990). *Spline models for observational data*. Society for Industrial Mathematics.
Winfree, A. T. (2001). *The geometry of biological time* (2nd ed.). Springer.